

Interstellar Dust in the Solar System: Model versus In-Situ Spacecraft Data

Harald Krüger (krueger@mps.mpg.de)¹; Peter Strub^{1,2}; Nicolas Altobelli³; Veerle Sterken⁴; Ralf Srama²; Eberhard Grün⁵

1) Max-Planck-Institut für Sonnensystemforschung, Göttingen, Germany; 2) Institut für Raumfahrtssysteme, Universität Stuttgart, Germany; 3) European Space Agency, ESAC, Madrid, Spain; 4) Institute of Applied Physics, University of Bern, Switzerland; 5) Max-Planck-Institut für Kernphysik, Heidelberg, Germany

Abstract

In the early 1990s, contemporary interstellar dust penetrating deep into the heliosphere was identified with the in-situ dust detector on board the Ulysses spacecraft. Later on, interstellar dust was also identified in the data sets measured with dust instruments on board Galileo, Cassini and Helios. Ulysses monitored the interstellar dust stream at high ecliptic latitudes for about 16 years. The three other spacecraft data sets were obtained in the ecliptic plane and cover much shorter time intervals. We compare in-situ interstellar dust measurements obtained with these four spacecrafts, published in the literature, with predictions of a state-of-the-art model for the dynamics of interstellar dust in the inner solar system (Interplanetary Meteoroid environment for EXploration, IMEX), in order to test the reliability of the model predictions. Micrometer and sub-micrometer sized dust particles are subject to solar gravity and radiation pressure as well as to the Lorentz force on a charged dust particle moving through the Interplanetary Magnetic Field, leading to a complex size dependent flow pattern of interstellar dust in the planetary system. The IMEX model was calibrated with the Ulysses interstellar dust measurements and includes these relevant forces. We study the time-resolved flux and mass distribution of interstellar dust in the solar system. The IMEX model agrees with the spacecraft measurements within a factor of 2 to 3, also for time intervals and spatial regions not covered by the original model calibration with the Ulysses data set. It usually underestimates the dust fluxes measured by the space missions which were not used for the model calibration, i.e. Galileo, Cassini and Helios. IMEX is a unique time-dependent model for the prediction of interstellar dust fluxes and mass distributions for the inner and outer solar system. The model is suited to study dust detection conditions for past and future space missions.

1 Introduction

Interstellar dust became a topic of astrophysical research in the early 1930s when astronomers realized the extinction of starlight in the interstellar medium (ISM). At that time, information about dust in the ISM could only be obtained by astronomical observations. With the advent of dust detectors onboard spacecraft in the 1970s, it became

possible to investigate dust particles in-situ, and the analysis of data obtained with the dust instruments flown on a couple of spacecraft suggested that interstellar dust can cross the heliospheric boundary and penetrate deep into the heliosphere (Bertaux and Blamont, 1976; Wolf et al., 1976, see Krüger and Grün (2009) for a review). Later on, in the 1990s, this was undoubtedly demonstrated by the Ulysses spacecraft: the Ulysses dust detector, which measured mass, speed and approach direction of the impacting particles, identified interstellar particles with radius above $0.1 \mu\text{m}$ sweeping through the heliosphere (Grün et al., 1993, 1994, 1995). These particles originated from the local interstellar cloud (LIC) surrounding our solar system (Frisch et al., 1999), thus providing an opportunity to probe dust from the LIC.

The motion of the heliosphere with respect to this cloud causes an inflow of interstellar dust into the heliosphere from a direction of 259° ecliptic longitude and 8° latitude (Landgraf, 1998; Frisch et al., 1999; Strub et al., 2015) with an inflow speed of 26 km s^{-1} (Grün et al., 1994; Krüger et al., 2015). Within the measurement accuracy, the average dust inflow direction is co-aligned with the interstellar neutral helium flow (Witte et al., 1996, 2004; Wood et al., 2015)¹. The interstellar dust flow persists at high ecliptic latitudes above and below the ecliptic plane and even over the poles of the Sun, whereas interplanetary dust is strongly depleted at high latitudes (Grün et al., 1997).

The Ulysses interstellar dust measurements were confirmed by the Galileo (Baguhl et al., 1996; Altobelli et al., 2005b) and Cassini spacecraft (Altobelli et al., 2003, 2007, 2016), and interstellar impactors were also identified in the Helios dust data (Altobelli et al., 2006). In 2006, the Stardust mission successfully brought a sample of collected interstellar particles to Earth (Westphal et al., 2014). Finally, measurements by the radio and plasma wave instruments on board the STEREO and WIND spacecraft were explained by interstellar dust (Belheouane et al., 2012; Malaspina and Wilson, 2016), although this interpretation was recently called into question (Kellogg et al., 2018).

Measurements of interstellar dust inside the planetary system now provide a window for the study of solid interstellar matter at our doorstep (Frisch et al., 1999). However, the flow of the interstellar particles in the heliosphere is governed by two fundamental effects: (1) the combined gravitational force and the radiation pressure force of the Sun, and (2) the Lorentz force acting on a charged particle moving through the solar magnetic field "frozen" into the solar wind. The former effect can be described as a multiplication of the gravitational force by a constant factor $(1 - \beta)$, where the radiation pressure factor $\beta = |\mathbf{F}_{rad}|/|\mathbf{F}_{grav}|$ is a function of particle composition, size and morphology. Interstellar particles approach the Sun on hyperbolic trajectories, leading to either a radially symmetric focussing ($\beta < 1$) or defocussing ($\beta > 1$) downstream of the Sun which is constant in time (Bertaux and Blamont, 1976; Landgraf, 2000; Sterken et al., 2012). Particle sizes observed by the Ulysses dust detector typically range from approximately $0.1 \mu\text{m}$ to several micrometers, corresponding to $0 \lesssim \beta \lesssim 1.9$ (Kimura et al., 2003; Landgraf et al., 1999)². A detailed description of the forces acting on the particles and the resulting general interstellar

¹Working values of a speed of 25.4 km s^{-1} with directions from 255.7° ecliptic longitude and $+5.1^\circ$ ecliptic latitude were suggested from Energetic Neutral Atom measurements by the Interstellar Boundary Explorer mission (IBEX) by McComas et al. (2015) and recently confirmed by Swaczyna et al. (2018).

²Landgraf et al. (1999) found a range of $1.4 < \beta < 1.8$ from Ulysses measurements, and Kimura et al.

dust flow characteristics was given by Sterken et al. (2012). Reviews about interstellar dust measurements in the solar system were recently given by Mann (2010) and Sterken et al. (2019).

The interplanetary magnetic field (IMF) shows systematic variations with time, including the 25-day solar rotation and the 22-year solar magnetic cycle, as well as local deviations caused by disturbances in the interplanetary magnetic field, due to, e.g. coronal mass ejections (CMEs). The dust particles in interplanetary space are typically charged to an equilibrium potential of +5 V (Kempf et al., 2004). Small particles have a higher charge-to-mass ratio, hence their dynamics is more sensitive to the interplanetary magnetic field. The major effect of the magnetic field on the charged interstellar dust is a focussing and defocussing relative to the solar equatorial plane with the 22-year magnetic cycle of the Sun (Landgraf, 2000; Landgraf et al., 2003; Sterken et al., 2012, 2013). Modifications of the particle dynamics by solar radiation pressure and the Lorentz force acting on charged dust particles have to be taken into account for a proper interpolation of the interstellar dust properties to the interstellar medium outside the heliosphere where these particles originate from.

Results of interstellar dust measurements and simulations (including mass distributions) from Galileo and Ulysses were compared and studied by Landgraf et al. (2000). A first comparison of the interstellar dust data obtained with four spacecraft, i.e. Ulysses, Galileo, Cassini and Helios, was performed by Altobelli et al. (2005a). The results showed a decrease of the measured flux in the inner solar system which was attributed to heliospheric filtering. However, no comparison with a detailed dynamical model for all four missions was possible at the time. Only for the Galileo and Ulysses (partial) data sets (Landgraf, 1998) and the (complete) Ulysses data set (Sterken et al., 2015), detailed comparisons have been made. Here we use these same data and compare them with simulation results obtained from our latest model for the dynamics of interstellar dust in the solar system (Landgraf, 2000; Sterken et al., 2013; Strub et al., 2019).

In Section 2 we briefly present the interstellar dust measurements obtained by the Helios, Cassini, Galileo and Ulysses missions. For a comprehensive description of the data analysis, in particular the identification scheme for the interstellar impactors, the reader is referred to the publications by Altobelli et al. (2003, 2005b, 2006, 2016) for Helios, Galileo and Cassini, and Strub et al. (2015) for the Ulysses data. In Section 3 we present our modelling results and compare them with the in-situ measurements. Section 4 is a Discussion and in Section 5 we summarise our conclusions.

2 In-Situ Spacecraft Dust Data

The physical mechanism most generally utilized in modern spaceborne in-situ dust detectors is based on the measurement of the electric charge generated upon impact of a fast projectile on to a solid target (impact ionization). It yields the highest sensitivity for the detection of dust particles in space (Fechtig et al., 1978; Auer, 2001). The impact can be detected by several independent measurements on different instru-

(2003) found values for β between 0 and 1.9

ment channels (multi-coincidence detection) which allows for a reliable dust impact detection and identification of noise events (Grün et al., 1992a). The electrical charge generated upon impact can be empirically calibrated to provide the impact speed and the mass of the particle (Göller and Grün, 1985). In combination with a time-of-flight mass spectrometer, an impact ionisation detector can measure the chemical composition of the impacting particle (Srama et al., 2004).

In this work we use dust data obtained by impact ionization dust detectors on board the spacecraft Helios, Galileo, Cassini and Ulysses (Dietzel et al., 1973; Grün, 1981; Grün et al., 1992a,b; Srama et al., 2004). Impacts of interstellar dust particles in these data sets were identified by Altobelli et al. (2006, 2005b, 2003, 2016) and Strub et al. (2015). We do not consider dust measurements with other detection techniques here because we want to keep the data set as consistent as possible. Different detection techniques are usually connected with individual systematic uncertainties, e.g. due to mass calibration or instrument detection threshold, increasing the overall uncertainty.

When a dust particle strikes a solid target with high speed ($\gg 1 \text{ km s}^{-1}$), it forms a crater in the target and releases ejecta composed of both particle and target material. The ejecta consist of positive and negative ions, electrons, and neutral atoms and molecules originating from both projectile and target. Because of its high internal pressure (up to 5 TPa), the ejecta cloud expands rapidly into the surrounding vacuum.

The sensors consist of a metal plate target and a collector (e.g. a metal grid) for either the ions or electrons of the impact plasma. Different electric potentials applied to the target plate and the collector generate an electric field, separating the positively and negatively charged ions. Charge-sensitive amplifiers coupled to both the target plate and the collector register independently, but simultaneously, an impacting dust particle. The total amount of charge, Q_{imp} , collected on each channel is a function of mass m_d and impact speed v_d of the particle as well as the particle's composition. Q_{imp} can be described by the empirical law

$$Q_{imp} = K m_d^\alpha v_d^\gamma, \quad (1)$$

with $\alpha \simeq 1$ and $1.5 \lesssim \gamma \lesssim 5.5$ in the speed range $2 \text{ km s}^{-1} \lesssim v \lesssim 70 \text{ km s}^{-1}$ (Auer, 2001; Stübig, 2002). K depends on the sensor geometry and the signal processing by the instrument electronics. In particular, for constant impact speed, the charge generated upon impact is proportional to the particle mass (Göller and Grün, 1985).

The instrument sensitivity, expressed by the parameter K , is determined by the technical detection threshold for the impact charge measurement, which is about 10^{-14} C for Ulysses, Galileo and Helios, and 10^{-15} C for Cassini, respectively. However, the interstellar impactors had to be separated from interplanetary particle impacts which was usually done by their impact direction and impact speed (or generated impact charge). This led to specific identification criteria for the interstellar particles in the data sets of the four space missions, and thus in most cases to less sensitive detection thresholds than the technically detectable threshold. The measurement periods of the different space missions, details of the particle identification schemes and derived dust fluxes are summarized in Table 1.

The particle speed can be determined from the rise times of the individual charge signals (Göller and Grün, 1989). For a given impact speed the signal strength also moderately depends on the particle material and on the impact angle. Neither the

Table 1: Characteristics of the individual spacecraft measurements.

Mission/ Interval	Start Time	End Time	Range	Impact Speed	$^{\dagger}Q_{imp}/m_d$	†† Detection Threshold			*N	* Average flux
(1)	[year-day]	[year-day]	[AU]	v_d [kms $^{-1}$]	[C/kg]	Charge Q_{imp} [C]	Mass m_d [kg]	Radius r_d [μ m]	(10)	[m $^{-2}$ s $^{-1}$]
(1)	(2)	(3)	(4)	(5)	(6)	(7)	(8)	(9)	(10)	(11)
Helios										
HEL**	1974-353	1980-002	0.3 – 1.0	60	$2.6 \cdot 10^3$	$2 \cdot 10^{-12}$	$7 \cdot 10^{-16}$	0.37	27	$(2.6 \pm 0.3) \cdot 10^{-6}$
Galileo										
GLL1	1990-001	1990-190	0.7 – 1.2	50	$5.0 \cdot 10^4$	$2 \cdot 10^{-12}$	$4 \cdot 10^{-17}$	0.14	21	$(7.0 \pm 1.5) \cdot 10^{-5}$
GLL2	1991-056	1991-123	1.0 – 1.4	50	$5.0 \cdot 10^4$	$2 \cdot 10^{-12}$	$4 \cdot 10^{-17}$	0.14	13	$(9.5 \pm 1.5) \cdot 10^{-5}$
GLL3	1991-228	1991-340	1.9 – 2.2	30	$6.5 \cdot 10^3$	$1 \cdot 10^{-13}$	$2 \cdot 10^{-17}$	0.11	19	$(3.5 \pm 0.8) \cdot 10^{-5}$
GLL4	1993-005	1993-181	1.2 – 2.5	50	$5.0 \cdot 10^4$	$2 \cdot 10^{-12}$	$4 \cdot 10^{-17}$	0.14	22	$(8.0 \pm 1.0) \cdot 10^{-5}$
GLL5	1993-182	1993-365	2.5 – 3.5	35	$1.1 \cdot 10^4$	$1 \cdot 10^{-13}$	$9 \cdot 10^{-18}$	0.09	41	$(2.5 \pm 0.5) \cdot 10^{-5}$
Cassini										
CAS1	1999-081	1999-181	0.7 – 1.2	45	$6.0 \cdot 10^4$	$3 \cdot 10^{-12}$	$5 \cdot 10^{-17}$	0.15	14	$(1.5 \pm 0.5) \cdot 10^{-4}$
CAS2***	2004-183	2013-364	9.1 – 9.9	30	$8.0 \cdot 10^3$	$1 \cdot 10^{-15}$	$5 \cdot 10^{-18}$	0.07	36	$(7.7 \pm 2.0) \cdot 10^{-5}$
Ulysses										
ULS1	1992-245	1994-131	3.0 – 5.0	30	$6.5 \cdot 10^3$	$1 \cdot 10^{-13}$	$2 \cdot 10^{-17}$	0.11	116	$(5.3 \pm 1.7) \cdot 10^{-5}$
ULS2	1995-166	1996-131	1.9 – 3.7	30	$6.5 \cdot 10^3$	$1 \cdot 10^{-13}$	$2 \cdot 10^{-17}$	0.11	39	$(2.9 \pm 1.1) \cdot 10^{-5}$
ULS3	1996-131	2000-131	3.7 – 5.4	30	$6.5 \cdot 10^3$	$1 \cdot 10^{-13}$	$2 \cdot 10^{-17}$	0.11	94	$(1.1 \pm 0.3) \cdot 10^{-4}$
ULS4	2002-131	2002-363	3.5 – 4.4	25	$4.0 \cdot 10^3$	$1 \cdot 10^{-13}$	$3 \cdot 10^{-17}$	0.13	37	$(1.1 \pm 0.2) \cdot 10^{-4}$
ULS5	2005-245	2006-245	3.2 – 4.9	30	$6.5 \cdot 10^3$	$1 \cdot 10^{-13}$	$2 \cdot 10^{-17}$	0.11	79	

Notes. Spacecraft (column 1), measurement periods (columns 2 and 3), heliocentric distance range (column 4), average interstellar dust impact speed derived from the model (column 5), charge-to-mass ratio from instrument calibration (column 6), detection thresholds (columns 7 to 9), number of identified interstellar particles (column 10), and average interstellar dust fluxes (column 11).

* Altobelli et al. (2006), Altobelli et al. (2005b), Altobelli et al. (2003), Strub et al. (2015)

** For Helios we have considered only impacts when the true anomaly angle of the spacecraft was in the range $-180^\circ < \nu < 90^\circ$ consistent with Altobelli et al. (2006).

*** Cassini CDA was not pointing into the direction of interstellar dust continuously during this time interval (Altobelli et al., 2016)

† Grün (1981); Grün et al. (1995); Stübig (2002)

†† Detection threshold based on the identification scheme for interstellar particles. Throughout this paper we calculate particle radii from the measured masses by assuming a spherical particle shape and a density typical of astronomical silicates $\rho_d = 3300 \text{ kg m}^{-3}$ (Kimura and Mann, 1999). The particle radius is given by

$$r_d = \sqrt[3]{\frac{3m_d}{4\pi\rho_d}}, \quad (2)$$

where m_d is the dust particle mass derived from the instrument calibration.

particle material nor the impact angle are known for an impinging particle. Therefore, averaged calibration curves have to be used to obtain impact speeds, assuming that the materials used for calibration represent cosmic dust particles (Grün et al., 1995). The typical accuracy of the derived speed v_d is a factor of 2.

Once the particle speed has been determined, its charge-to-mass ratio Q_{imp}/m_d generated upon impact can be derived from empirical calibration curves. These were obtained from impact experiments at the dust accelerator facility at Max-Planck-Institut für Kernphysik, Heidelberg (γ in Equation 1; Grün, 1981; Grün et al., 1995; Stübig, 2002; Srama et al., 2004; Srama, 2009). In the next step, the particle mass can be derived from the calibrated impact charge-to-mass ratio and the measured impact charges. If the speed is well determined, the mass can also be derived with a higher accuracy. The typical uncertainty in the derived mass m_d is a factor of 10.

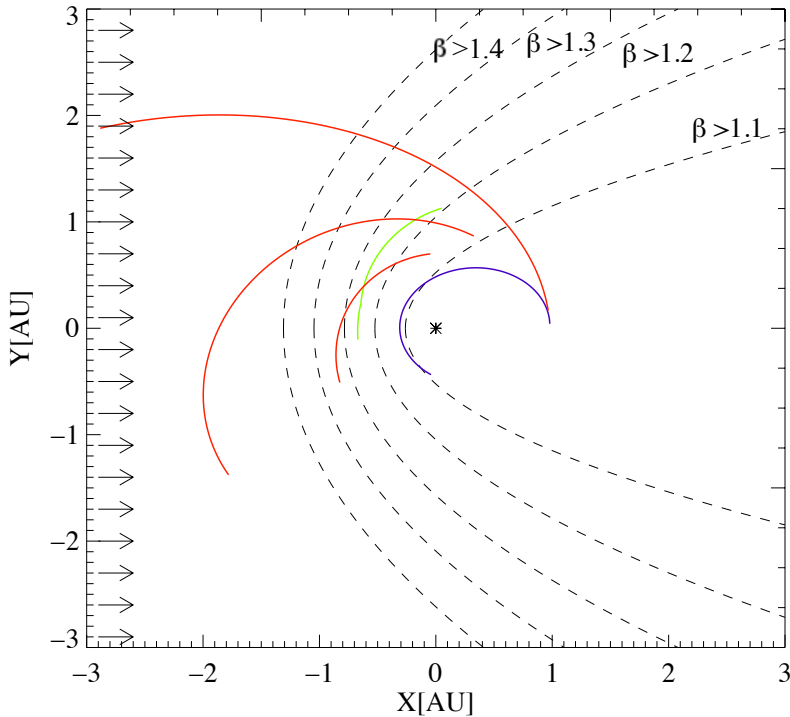


Figure 1: Trajectory segments of Helios (blue), Galileo (red), and Cassini (green) which were favorable for the identification of interstellar dust. The Sun is at the center and the X-Y plane is the ecliptic plane. Vernal equinox is approximately towards the -Y direction, and the nominal interstellar dust flow direction is indicated by arrows. Different β avoidance cones are indicated by dashed lines. See text for details.

Given that the charge-to-mass ratio Q_{imp}/m_d strongly depends on particle impact speed, we had to assume a speed in order to derive the particle mass from the measured impact charge in the spacecraft data (Equation 1). For our analysis we took average particle speeds from the model for the measurement time interval considered (Section 3), and the corresponding Q_{imp}/m_d listed in Table 1.

2.1 Helios

The Helios 1 spacecraft (we refer only to Helios 1 throughout this paper) was launched into a heliocentric orbit on 10 December 1974, with perihelion and aphelion distances of 0.3 AU and 1.0 AU, respectively (Figure 1). The spacecraft was spin-stabilized with a spin axis pointing normal to the ecliptic plane and a spin period of one second. It carried two dust instruments, the ecliptic sensor which was exposed to sunlight, and the south sensor which was shielded by the spacecraft from direct sunlight (Dietzel et al., 1973; Fechtig et al., 1978; Grün, 1981; Altobelli et al., 2006).

Between 19 December 1974 and 2 January 1980 the Helios sensors transmitted the data of 235 dust impacts to Earth (Grün, 1981). Interstellar impactors could only be separated from interplanetary dust particles if their impact charge exceeded $2 \cdot 10^{-12} \text{ C}$

and only during limited periods of the Helios orbit. This led to the identification of 27 interstellar impactors during ten orbits of Helios around the Sun when the spacecraft's true anomaly angle ν was in the range $-180^\circ < \nu < 90^\circ$ (Altobelli et al., 2006). Calibration parameters $K = 4.07 \cdot 10^{-5}$ (mass taken in gram) and $\gamma = 2.7$ (Grün, 1981) were used, and the derived particle masses were mostly in the range $10^{-15} \text{ kg} \lesssim m_d \lesssim 10^{-14} \text{ kg}$. Details of the Helios measurements are summarized in Table 1.

In addition to measuring particle masses and fluxes, the instruments performed a low-resolution compositional analysis with a time-of-flight analyser (Auer, 2001). The Helios dust analyzers were the first instruments measuring the elemental composition of dust particles in interplanetary space.

2.2 Galileo

Galileo was launched on 18 October 1989, and after two flybys at Earth and one at Venus the spacecraft had enough energy to reach Jupiter in December 1995. Galileo was the first spacecraft in orbit about Jupiter until the mission was terminated on 21 September 2003. Galileo was a dual-spinning spacecraft, with the dust detector mounted on the despun section of the spacecraft. The Galileo dust detector measured dust particle flux, impact direction, speed and mass of the impacting particles (Grün et al., 1992a). It was a twin of the dust detector on board Ulysses (Grün et al., 1992b).

During Galileo's interplanetary mission three orbit segments had a detection geometry which allowed the identification of interstellar dust (Figure 1). Due to the varying impact speeds, different charge detection thresholds apply to these intervals (corresponding to impact charge thresholds ranging from $1 \cdot 10^{-13} \text{ C}$ to $2 \cdot 10^{-12} \text{ C}$, cf. Table 1). A total of 115 interstellar impactors were identified in the Galileo data set (Altobelli et al., 2005b). For our analysis we have split the three orbit segments shown in Figure 1 into five time intervals. The mass calibration was obtained from an empirical calibration curve (Grün et al., 1995, their Figure 3a).

2.3 Cassini

The Cassini spacecraft was launched on 15 October 1997. During its first two years in interplanetary space the spacecraft performed two flybys at Venus and one at Earth to gain enough energy to reach Saturn. In 2004 it became the first spacecraft in orbit about the giant ring planet, until the mission was terminated on 15 September 2017. Cassini was a 3-axis stabilized spacecraft.

The Cassini Cosmic Dust Analyzer (CDA) was an upgrade of the dust detectors flown on board Galileo and Ulysses, measuring particle composition and electric charge in addition to particle mass, impact speed, flux and direction (Srama et al., 2004). For CDA we use the mass calibration derived by Stübig (2002, his Figure 5.1).

Due to operational constraints of the Cassini spacecraft during its interplanetary voyage, interstellar dust particles could only be measured during approximately three months from 22 March 1999 to 30 June 1999 at a heliocentric distance between 0.7 AU and 1.2 AU (Figure 1). A charge detection threshold of $3 \cdot 10^{-12} \text{ C}$ had to be used in this period, and 14 ± 3 particle impacts of likely interstellar origin were identified in

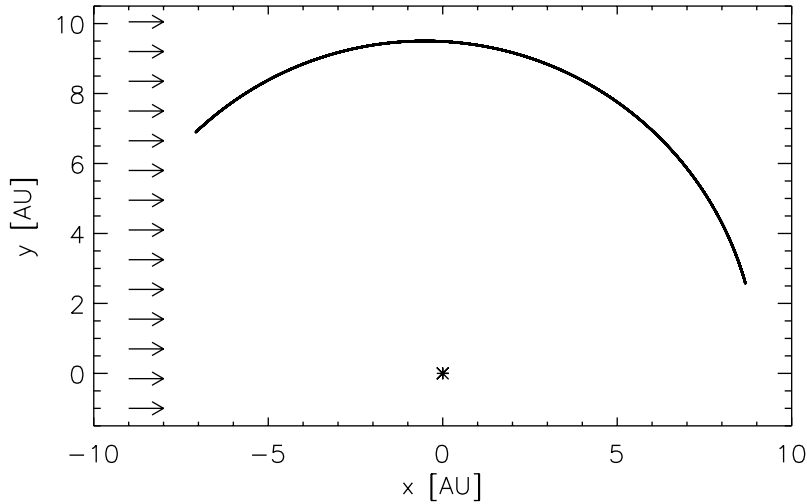


Figure 2: Same as Figure 1 but for Cassini at Saturn.

the mass range $5 \cdot 10^{-17} \text{ kg} \leq m_d \leq 10^{-15} \text{ kg}$ (Altobelli et al., 2003). Details of the Cassini measurements can be found in Table 1.

The Cassini CDA instrument detected interstellar dust also in the Saturnian system (Altobelli et al., 2016, Figure 2). A total of 36 interstellar particles were identified within a distance range of 9 to 60 Saturn radii from the planet by their high entry speed into the Saturnian system and their impact direction which was compatible with the expected interstellar dust flow direction at Saturn. The derived average particle flux was $1.5 \cdot 10^{-4} \text{ m}^{-2} \text{ s}^{-1}$ in the mass range $5 \cdot 10^{-18} \text{ kg} \leq m_d \leq 5 \cdot 10^{-16} \text{ kg}$.

Impacts onto the CDA Chemical Analyzer Target by sufficiently large particles do not provide time-of-flight spectra with sufficiently well resolved spectral lines from which the minimum impact speed can be derived. The Cassini 2 measurement interval therefore lacks particles heavier than approximately $5 \cdot 10^{-16} \text{ kg}$.

From the rise time of the impact charge signals the particle impact speed can usually be determined with a factor of 2 uncertainty. The shape of the time-of-flight mass spectra produced by the CDA Chemical Analyzer Target (CAT), however, provides a more accurate determination of the minimum impact speed of each impactor. This method, therefore, being based on the velocity-mass calibration for the CAT, also provides a better estimate of the upper mass value for each impactor (compared to the factor of ten, see Section 2 above). The time-of-flight mass spectra method also yields a lower dust detection statistics, compared to measurements performed by the dust instruments on-board Ulysses and Galileo, because of the smaller CAT surface.

2.4 Ulysses

Ulysses was launched on 6 October 1990. During a flyby at Jupiter on 8 February 1992 it was deflected on to an orbit almost perpendicular to the ecliptic plane and it became the first spacecraft on a polar orbit about the Sun. Operations of Ulysses were

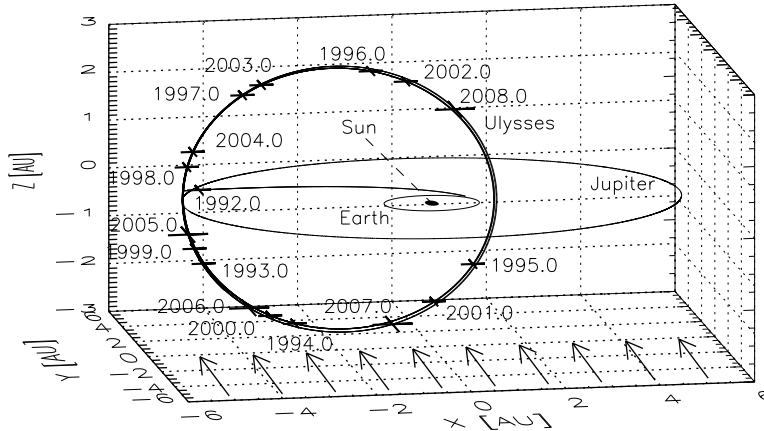


Figure 3: Trajectory of Ulysses in ecliptic coordinates with the Sun at the center. The orbits of Earth and Jupiter indicate the ecliptic plane, and the initial trajectory of Ulysses was in this plane. After Jupiter flyby in early 1992, the orbit was almost perpendicular to the ecliptic plane (79° inclination). Crosses mark the spacecraft position at the beginning of each year. Vernal equinox is to the right (positive x-axis). Arrows indicate the nominal interstellar dust flow direction, which is within the measurement accuracy co-aligned with the direction of the interstellar helium gas flow. It is almost perpendicular to the orbital plane of Ulysses.

terminated on 29 June 2009. The dust detector on board (Grün et al., 1992b) was a twin of the Galileo dust detector. Ulysses was a spinning spacecraft with a period of 5 revolutions per minute. The Ulysses trajectory is shown in Figure 3.

The Ulysses mission was particularly well suited for the detection of interstellar particles. First, its highly inclined orbit with an aphelion at approximately Jupiter's orbit (5.5 AU) took the spacecraft far above the ecliptic plane. Given that the concentration of interplanetary dust particles drops at increasing ecliptic latitudes and that most of the interplanetary dust moves on prograde heliocentric orbits, the orbital sections where Ulysses was far from its perihelion and far from the solar poles were best suited for the detection of interstellar dust. The orientation of Ulysses's orbital ellipse was such that in these sections the impact directions of interplanetary and interstellar particles were almost antiparallel, and thus these populations could easily be separated.

The Ulysses dust data is by far the largest data set of in-situ interstellar dust measurements available to date. A detection threshold of $1 \cdot 10^{-13}$ C had to be used and the data set contains more than 900 identified interstellar particles, covering about 75% of one full 22-year solar cycle (Strub et al., 2015; Krüger et al., 2010, 2015). For our analysis we have selected five mission intervals when the dust detector was continuously measuring dust (cf. Table 1). Similar to Galileo, the mass calibration was obtained from an empirical calibration curve (Grün et al., 1995, their Figure 3a). Given the long time coverage and thus large number of identified interstellar parti-

cles, the dust model we are going to use in Section 3 was calibrated with the Ulysses interstellar dust data set (Strub et al., 2019).

3 Interstellar Dust Simulations

Previous models for interstellar dust in the solar system described the interstellar dust flow at larger heliocentric distances well, but they did not have the resolution to enable a good time-resolved description of the dust environment at Earth (Grün et al., 1994; Landgraf, 2000; Sterken et al., 2012). Based on these earlier models and the dust measurements by the Ulysses spacecraft, Strub et al. (2019) executed high-resolution simulations in the context of the IMEX modelling effort (Interplanetary Meteoroid environment for EXploration) that included an interstellar dust module developed for this purpose. The authors simulated the dynamics of charged micrometer and sub-micrometer sized interstellar particles exposed to solar gravity, solar radiation pressure and a time-varying IMF. The mass distribution is represented by 12 particle sizes between $0.049 \mu\text{m}$ and $4.9 \mu\text{m}$, and the dynamics of each of these sizes was simulated individually.

In IMEX the dust density in the solar system is calibrated with the Ulysses interstellar dust measurements which is by far the most comprehensive data set of interstellar dust measurements presently available (Strub et al., 2015; Krüger et al., 2015). Each particle size bin in the model was calibrated such that the average dust flux measured by Ulysses in this size bin was reproduced (Strub et al., 2019). Due to the variation of the IMF imposed by the 22-year solar cycle, the model is time-dependent. For details of the model and general interstellar dust flow characteristics the reader is referred to Sterken et al. (2012), and for the flow at Earth orbit to Strub et al. (2019). Here we use IMEX to simulate dust fluxes and we compare the results with the dust measurements discussed in Section 2.

Throughout this paper we use the inflow direction of the interstellar dust into the heliosphere from a direction of 259° ecliptic longitude and 8° latitude and inflow speed of 26 km s^{-1} as the nominal direction and speed of the undisturbed interstellar dust flow. This is equivalent to the interstellar particles being at rest with respect to the local interstellar cloud, and they approach the Sun on hyperbolic trajectories. The trajectories of particles with $\beta = 1$ are altered neither by solar radiation nor by solar gravity. The only force leading to a deflection of these particles is the Lorentz force imposed by the IMF. For particles with $\beta \neq 1$ the solar radiation pressure leads to either a concentration of particles ($\beta < 1$) downstream of the Sun, or to a deflection ($\beta > 1$) and thus to a time-independent depletion cone downstream of the Sun (Figure 1).

In our model, the dynamics of particles with approximate radii $0.1 \mu\text{m} \lesssim r_d \lesssim 0.5 \mu\text{m}$ are dominated by solar radiation pressure, larger particles are dominated by gravity, and smaller particles by the Lorentz force imposed by the IMF. The β -mass relation used for each particle size in our simulations is determined according to the “adapted astronomical silicates β -curve” (Sterken et al., 2012) which combines the radiation pressure efficiencies of Gustafson (1994) with an average of the maximum values for β from Ulysses observations ($\beta = 1.6$, from Landgraf et al., 1999).

The time-variable IMF evolves through focussing and defocussing configurations

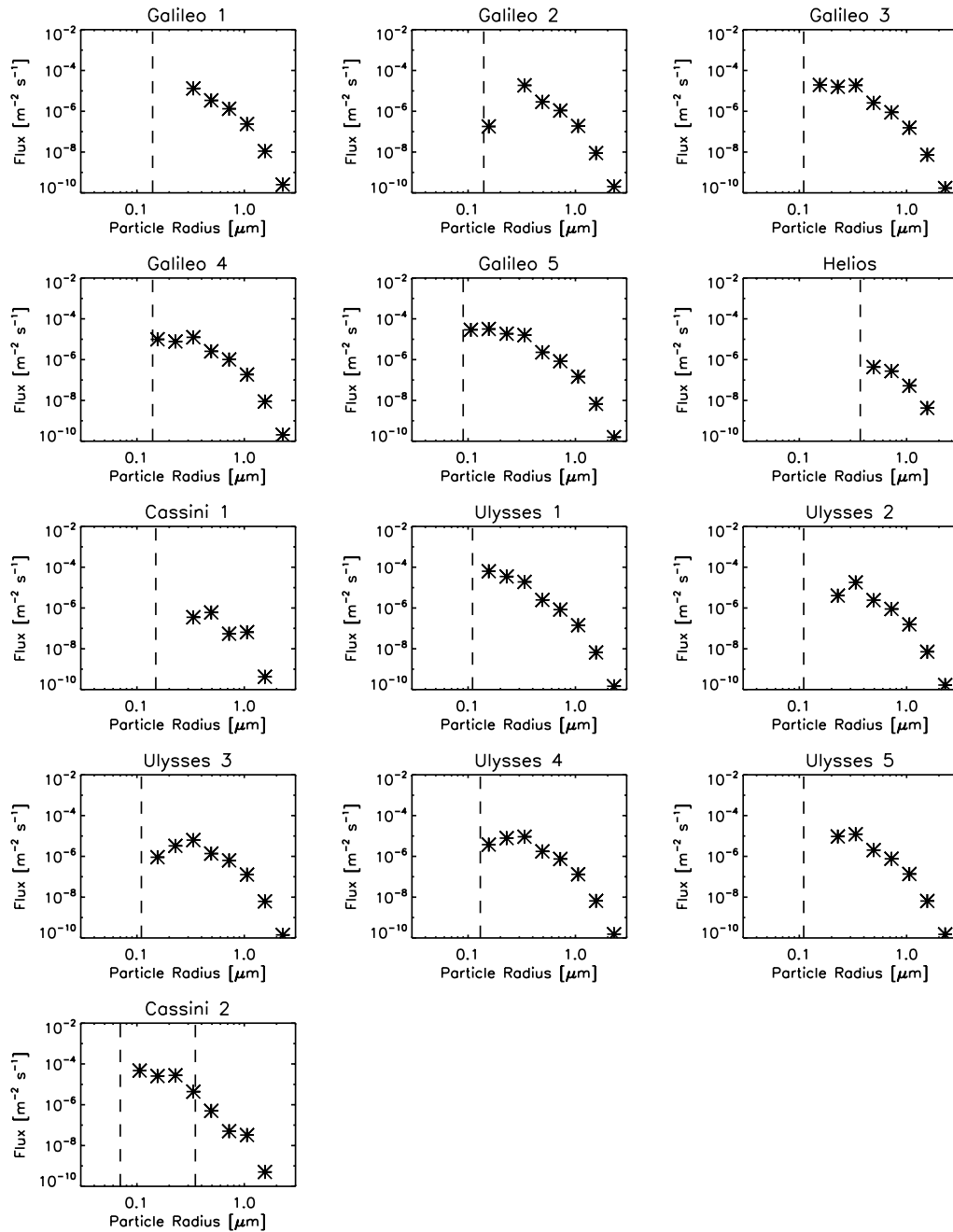


Figure 4: Interstellar particle size distributions obtained from the simulations for the different missions and orbit segments given in Table 1. Dashed vertical lines indicate the detection thresholds of the dust instruments assuming an average particle impact speed derived from the model, as discussed in Section 2 (columns 5 and 9 in Table 1). For the Cassini 2 interval the upper detection limit at approximately $0.35 \mu\text{m}$ particle radius for the CDA Chemical Analyzer Target is also shown.

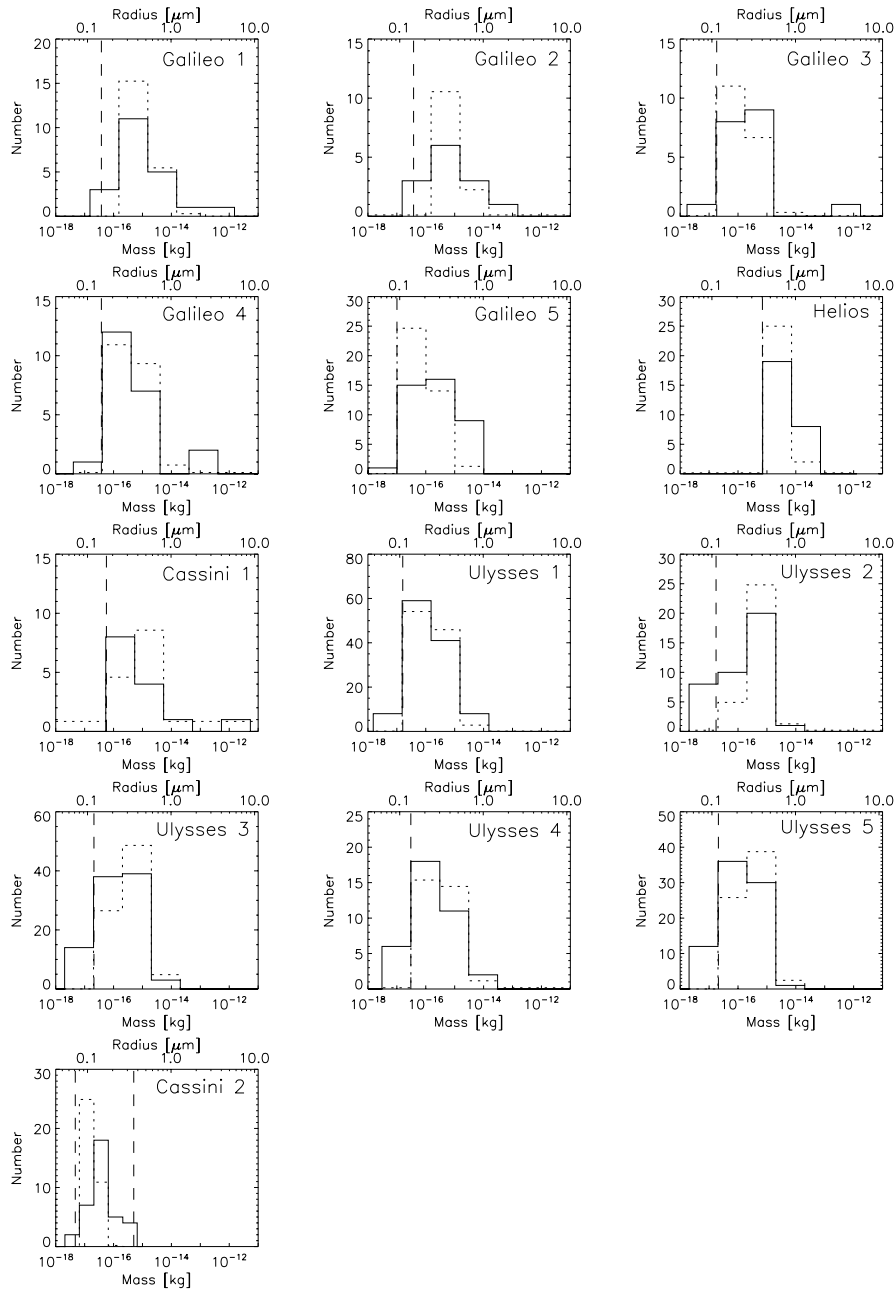


Figure 5: Mass distributions of interstellar impactors derived from the instrument calibration with the calibration parameters listed in Table 1 (solid histograms; from Altobelli et al. (2005b, 2003, 2006, 2016); Strub et al. (2015)). Dashed histograms show the fluxes shown in Figure 4 derived from the model. The model curves are normalized such that they contain the same number of particles as measured by the spacecraft detector in the time interval under consideration. Vertical dashed lines indicate the detection threshold assuming an average particle impact speed derived from the model (columns 5 and 9 in Table 1); for the Cassini 2 interval the upper detection limit for the CDA Chemical Analyzer Target is also shown. Particle radii are indicated at the top.

during the 22-year solar cycle. This causes time-dependent concentrations and rarefactions of interstellar particles smaller than approximately $0.3 \mu\text{m}$ in the inner solar system. We use the solar cycle approximation used by Strub et al. (2019, their Figure 1). Around the solar minima in 1974 and 1996, the IMF was in a defocussing configuration and around the solar minima in 1985 and 2007 the IMF was in a focussing configuration for these small particles.

We did not take into account the sensitivity profiles of the individual dust instruments. Instead, the model assumes a spherical sensor with 4π sensitivity characteristics, i.e. all particles reaching the spacecraft are taken into account. Given that for all space missions under consideration the dust sensors had a rather wide field-of-view and the interstellar dust flow is rather collimated, this is a reasonable approximation.

3.1 Dust Size Distributions

The simulated interstellar dust size distributions for the measurement periods of the four spacecraft considered here are shown in Figure 4. Vertical dashed lines indicate the detection thresholds which had to be applied to separate interstellar particles from other dust populations in the data sets (Altabelli et al., 2003, 2005b, 2006, 2016; Strub et al., 2015). Thus, interstellar particles to the left of the dashed lines – if present – could not be extracted from the data. Therefore, to avoid confusion in the following discussion, we do not show particles in this size range in Figure 4 even though they may be present in the model.

Strong variations are imposed by the varying heliocentric distances of the spacecraft and the time-dependent IMF configuration. The smallest particles are most effectively prevented from entering the inner solar system during defocussing configurations of the IMF. This leads to a strong depletion of particles smaller than approximately $0.3 \mu\text{m}$, in particular when the Helios and Cassini measurements were taken in the innermost regions of the solar system (cf. Table 1). Furthermore, particles in the size range $0.1 \mu\text{m} \lesssim r_d \lesssim 0.5 \mu\text{m}$ are depleted by the solar radiation pressure. Similarly, the Ulysses measurements 2 to 5 were taken during the defocussing configuration and are thus also strongly depleted in small particles. On the other hand, the Galileo intervals 1 to 3 were in the focussing phase of the IMF when small particles could reach the inner solar system.

In Figure 5 we compare the simulated dust mass distributions with the spacecraft measurements (the conversion between particle mass and radius is done with Equation 2, see footnote of Table 1). Again, the detection thresholds are indicated (Table 1, column 8). Particle masses were calculated from the measured impact charges with the average particle impact speeds derived from the simulations (Table 1, column 5), in the same way as the instrument detection thresholds.

In general, the masses predicted by the IMEX model are in good agreement with the measurements, only the Ulysses data show some impacts below the calculated detection thresholds. This is likely due to uncertainties in the mass calibration and/or the detection threshold. Note that, particle masses were derived from the measured impact charge using Equation 1 with a typical factor of 10 uncertainty in the mass calibration. Furthermore, all impacts were calibrated with the same average impact speed derived from the model, while the model predicts a speed variation of about

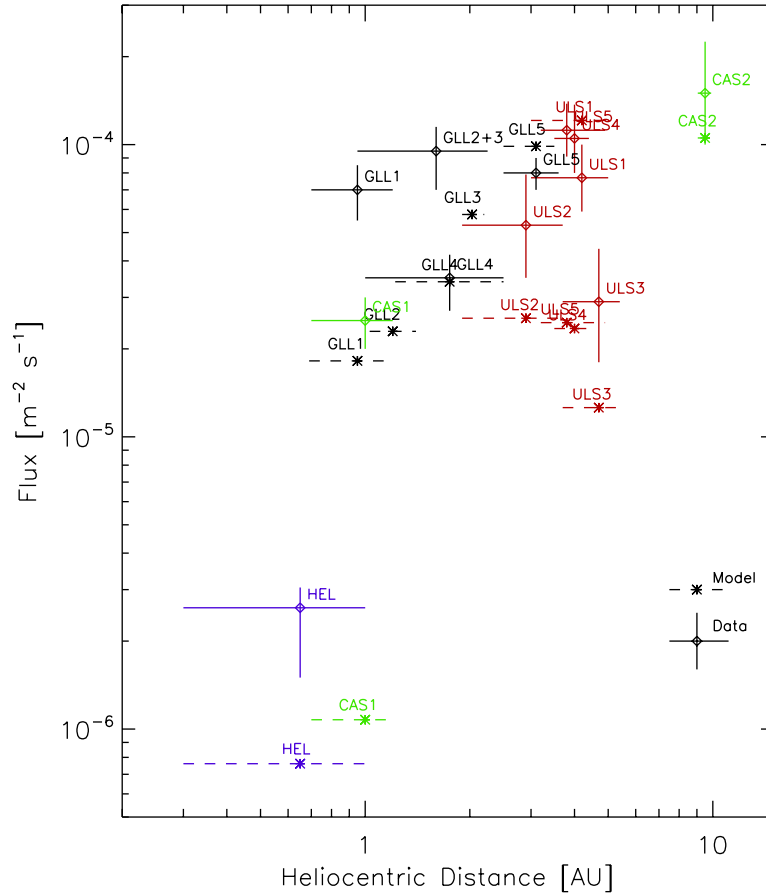


Figure 6: Dust fluxes simulated with IMEX (asterisks) and measured (diamonds) with Helios (HEL), Galileo (GLL), Cassini (CAS) and Ulysses (ULS). Horizontal bars indicate the distance range where dust measurements and simulations were performed. The detection thresholds and measured particle size ranges listed in Table 1 and shown in Figure 4 have been adopted for the simulations.

a factor of two during each of the measurement intervals. For the second Cassini interval, the minimum impact speed was derived from the impact spectra with a typical accuracy of 5 km s^{-1} , leading to a higher accuracy in the mass calibration. Thus, the data in Figure 5 are binned in intervals with one order of magnitude bin width, except for Cassini 2 where we achieved a higher mass resolution (cf. Section 2.3).

3.2 Dust Fluxes

In Figures 6 and 7 we show the simulated dust fluxes integrated over all detectable particle sizes and compare them with the measurements. We added up simulated fluxes for sizes only above the detection threshold shown in Figure 4 because smaller particles were not detectable by the dust instruments. The simulations were performed

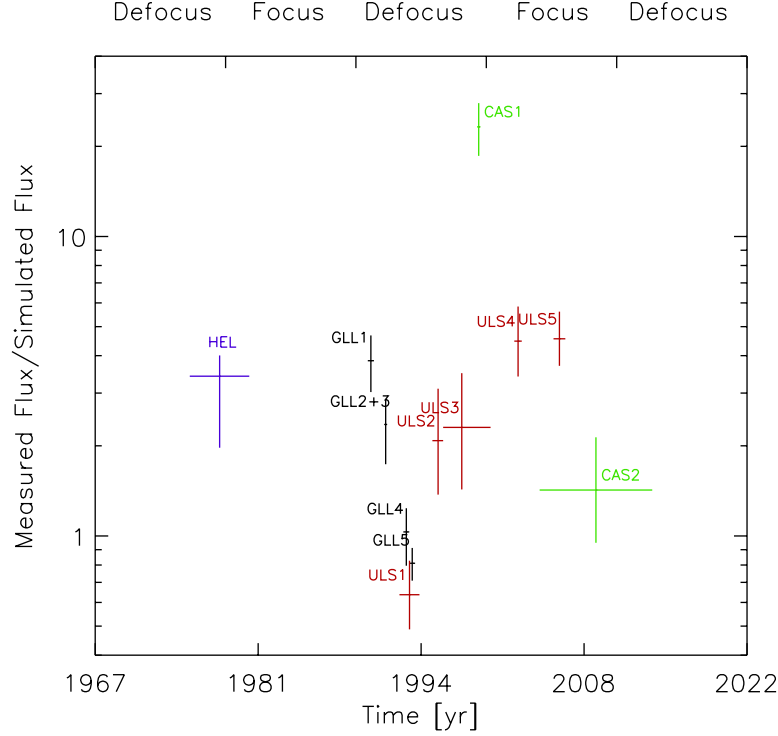


Figure 7: Ratio of measured to simulated dust fluxes from Figure 6. Horizontal bars indicate the time intervals when dust measurements and simulations were performed. The modelled focussing and defocussing phases of the IMF in the inner solar system based on observations by the Wilcox Solar Observatory (Hoeksema, 2018) are indicated at the top (Strub et al., 2019).

for the same time intervals as the measurements (columns 2 and 3 in Table 1). All measured and simulated dust fluxes discussed in this paper are given in the heliocentric reference system.

The model predicts on average somewhat lower fluxes than measured. This is also the case for Ulysses, even though the Ulysses data were used to calibrate the IMEX model. We will come back to this in Section 4. The mean value of the ratio between measured and simulated fluxes for Galileo, Cassini and Helios is $2.6^{+5.5}_{-1.7}$ (for all measurements including Ulysses it is $2.5^{+4.0}_{-1.5}$, 1σ uncertainty). If we ignore the data point for Cassini 1 we get a mean value of $1.8^{+1.7}_{-0.8}$ (without Ulysses).

4 Discussion

The IMEX model has been calibrated with the Ulysses interstellar dust data set because it is the most comprehensive and homogeneous measurement by a single dust instrument over a period of 16 years, covering a large portion of a full 22-year solar cycle (Figure 7). With more than 900 identified interstellar particles it has the best

statistical accuracy of all interstellar dust measurements with a dedicated dust detector obtained to date. For three of the five Ulysses measurement intervals the model reproduces the data within a factor of 2. Only after 2002 is the discrepancy somewhat more pronounced.

Given that the Ulysses data set was used to calibrate the IMEX model, this discrepancy is surprising at first glance. However, the model was calibrated with the full Ulysses data set, and it reproduces the overall interstellar dust fluxes measured during the entire mission to within 2%. This makes us very confident that the overall calibration of the model consistently reproduces the Ulysses measurements.

For the analysis in this paper we have used five relatively short time intervals for Ulysses instead of the full mission data set, mainly for two reasons: (1) we wanted to have a comparable number of dust impact events in each time interval as is the case for the other missions considered in this paper, and (2) we wanted to cover shorter heliocentric distance ranges than the entire Ulysses mission. Furthermore, we ignored the spatial region in the vicinity of Jupiter to make sure that we do not have a contamination by Jupiter stream particles (Krüger et al., 2006). Thus, we disregarded the time period from 2003 to mid 2005. It is not surprising that we get a somewhat larger discrepancy between model and data for shorter time intervals even though the model agrees very well with the data for the full time period.

The IMEX model reproduces most of the Galileo, Helios and Cassini measurements to within a factor of 2 to 3. Only during the Cassini 1 interval is the measured flux larger by approximately a factor of 20 than predicted by the model. It should be noted that the model as calibrated with the Ulysses data shows a tendency to predict *lower* fluxes than measured by the space instruments.

The underestimation of the flux in the Cassini 1 time interval may be related to the representation of the IMF by a Parker model (Strub et al., 2019): the Parker model describes the quiet IMF during solar minimum rather well, the Cassini 1 measurements, however, were performed around solar maximum during the strongest IMF defocussing conditions. Large deviations from the Parker IMF have to be expected, for example, inside CMEs which are not accounted for by the model. They can lead to severe discrepancies with the simulated flux.

Furthermore, discrepancies between model and data may be related to the demonstration by Sterken et al. (2015) that either the first part of the data (before 2002) or the last part (2002-2008) can be well represented by simulations of one dust population (size and physical properties) but not both periods in one simulation with a single set of particle properties. In 2005 a rapid change in interstellar flow direction and density was seen in the Ulysses data (Krüger et al., 2007), while in 2006 the flow direction was again co-aligned with the nominal flow direction of the interstellar helium within the measurement accuracy (Strub et al., 2015). The authors concluded that this was a temporally limited phenomenon. Sterken et al. (2015) simulated this shift in dust direction (i.e. the data after 2002) for porous bigger particles ($\gtrsim 0.2 \mu\text{m}$ radius) and for rather compact smaller ($\lesssim 0.2 \mu\text{m}$) particles. An extra (solar-cycle dependent) filtering mechanism in the outer boundary regions of the heliosphere (Kimura and Mann, 1998) included in the simulations may lead to a better fit for the entire Ulysses data set, in particular to reproduce the shift in dust flow direction in 2005.

The Ulysses measurements which were used for the model calibration covered the

time period from 1992 to 2007, a spatial region between approximately 2 AU and 5 AU, and they were acquired most of the time far away from the ecliptic plane (Strub et al., 2015; Krüger et al., 2015). The measurements by the other spacecraft were obtained in the ecliptic plane, at distance ranges much closer to the Sun inside Earth's orbit (Helios, Galileo and Cassini 1), further away from the Sun at Saturn (Cassini 2), or many years before Ulysses (Helios). The model shows overall good agreement with all these dust measurements, in particular those obtained in spatial regions not used for the model calibration.

All interstellar dust measurements obtained by Helios, Galileo and Cassini were obtained in the ecliptic plane in environments where solar-system dust populations dominate the particle fluxes: interplanetary dust particles dominate during all measurement intervals of these missions, while Saturnian dust makes an additional significant contribution in the Cassini 2 interval. Only Ulysses had an ideal configuration for interstellar dust detection far away from the ecliptic plane most of the time. Therefore, the interstellar dust measurement of Helios, Galileo and Cassini are connected with larger uncertainties in the particle identification and, hence, dust fluxes than those of Ulysses.

For Ulysses the selection criteria for the identification of interstellar particles in the data set used in this work are the same as the ones that were used by Strub et al. (2015) to analyze the dynamical properties of the particles. Krüger et al. (2015) used different criteria to derive the mass distribution of the particles in order not to induce any bias in the mass distribution. With their technique, these authors identified interstellar particles as small as $2 \cdot 10^{-18}$ kg in the Ulysses data set. It indicates that even though such small particles are strongly filtered by the heliospheric interaction, a fraction of them can still reach the inner solar system between 2 AU and 5 AU.

In Figure 5 the mass distributions measured by Ulysses are well reproduced by the model. On the other hand, the model overestimates the abundance of small particles close to the detection thresholds for a few of the Galileo measurement intervals and for Helios. In the future we may include these other dust measurements (Galileo, Cassini and Helios) to calibrate the model. This may improve the overall agreement between model and data for the dust fluxes and mass distributions. It is, however, beyond the scope of our present paper.

The Cassini measurements at Saturn (Cassini 2) show a deficit of small particles with masses below approximately $2 \cdot 10^{-17}$ kg (Figure 5), despite the fact that the sensitivity of the instrument enables the detection of smaller particles down to $5 \cdot 10^{-18}$ kg (Altobelli et al., 2016). This can be explained by the filtering of such small particles at the heliopause and the inner heliosphere (Sterken et al., 2013; Slavin et al., 2012), a phenomenon also observed in the Ulysses interstellar dust data (Landgraf, 2000). Furthermore, Altobelli et al. (2016) confirm the existence of particles with $\beta > 1$ with a maximum value reached between 10^{-17} kg and 10^{-16} kg, in good agreement with the β -mass domains inferred from the Ulysses data (Landgraf et al., 1999; Kimura et al., 2003).

The lack of large interstellar particles in the Cassini 2 data is due to the detection method on the CDA Chemical Analyzer Target (CAT): large impacts, typically micron-sized particles, do not provide time-of-flight spectra with sufficiently well resolved spectral lines from which the minimum impact speed can be derived. Further-

more, the almost ten times smaller CAT target area compared to the detection area of the Ulysses and Galileo instruments strongly reduces the likelihood of large particle detections.

Figure 6 shows an overall increase in the dust fluxes as a function of heliocentric distance. The detection thresholds varied for the different missions and measurement intervals, nevertheless this trend illustrates the filtering of the interstellar dust particles by the heliosphere. It confirms the earlier results by Altobelli et al. (2005a) which were based on a smaller data set and on the measurements alone, i.e. without modelling.

Finally, the ratio between measured and simulated fluxes in Figure 7 does not show a systematic trend with the solar cycle. It indicates that the description of the heliospheric filtering by the IMF implemented in the model is rather reliable.

The decrease in measured vs. simulated flux around 1994 may be caused by the filtering effect of the heliospheric boundary which is not yet implemented in the model. This was illustrated by Sterken et al. (2015, their Fig. 19): Particles passing through the solar system in 1994 have passed the boundary regions of the heliosphere in the defocusing phase of the solar cycle. In this region, higher particle charges (Kimura and Mann, 1998; Slavin et al., 2012) lead to larger Lorentz forces, thus filtering out interstellar dust particles, despite of a lower magnetic field strength in comparison with the solar system IMF. While Sterken et al. (2015) suggested this hypothesis for explaining the Ulysses data, here also the Galileo data (GLL4 and GLL5) seem to follow this trend. Further analysis is needed for confirmation.

The overall agreement between model and data indicates that an extrapolation of the model in space and time should, in general, give reliable predictions for future space missions with a tendency to underestimate the expected dust fluxes. The IMEX model was recently used to study the dust detection conditions for the DESTINY⁺ mission which will measure dust in interplanetary space between 2024 and 2028 and during a dedicated flyby at the active asteroid (3200) Phaethon (Kawakatsu and Itawa, 2013; Krüger et al., 2019; Kimura et al., 2019; Szalay et al., 2019).

5 Summary

We have used the interstellar dust module of the Interplanetary Meteoroid environment for EXploration model (IMEX; Sterken et al., 2013; Strub et al., 2019) to simulate the dynamics of interstellar dust in the solar system. The model covers all relevant forces, i.e. solar gravity, solar radiation pressure, and electromagnetic interaction with the interplanetary magnetic field. We have compared our model results with in-situ interstellar dust measurements obtained with four spacecraft, i.e. Helios, Galileo, Cassini, and Ulysses (Altobelli et al., 2006, 2005b, 2003, 2016; Strub et al., 2015). Our results can be summarized as follows:

The model gives overall good agreement with the spacecraft measurements. Dust fluxes and size distributions simulated for time intervals and spatial regions not covered in the original calibration of the model agree with the in-situ spacecraft measurements to within a factor of 2 to 3. This marks the limit of our current understanding of the interstellar dust flow through the solar system. The model usually underestimates the dust fluxes measured by spacecraft.

IMEX is a unique time-dependent model for the prediction of interstellar dust fluxes and mass distributions for the inner and outer solar system. The model is suited to study dust detection conditions for past and future space missions.

Acknowledgements

The IMEX model was developed under ESA funding (contract 4000106316/12/NL/AF - IMEX). H.K. and P.S. are grateful to the MPI für Sonnensystemforschung and the University of Stuttgart for their support. We are grateful to an anonymous referee whose comments substantially improved the presentation of our results.

References

- Altobelli, N., Dikarev, V., Kempf, S., Srama, R., Helfert, S., Moragas-Klostermeyer, G., Roy, M., and Grün, E. (2007). Cassini/Cosmic Dust Analyzer in situ dust measurements between Jupiter and Saturn. *Journal of Geophysical Research*, 112:7105.
- Altobelli, N., Grün, E., and Landgraf, M. (2006). A new look into the Helios dust experiment data: presence of interstellar dust inside the Earth’s orbit. *Astronomy and Astrophysics*, 448:243–252.
- Altobelli, N., Kempf, S., Krüger, H., Landgraf, M., Srama, R., and Grün, E. (2005a). In-Situ Monitoring of Interstellar Dust in the Inner Solar System. In *AIP Conf. Proc. 761: The Spectral Energy Distributions of Gas-Rich Galaxies: Confronting Models with Data*, pages 149–152.
- Altobelli, N., Kempf, S., Krüger, H., Landgraf, M., Roy, M., and Grün, E. (2005b). Interstellar dust flux measurements by the Galileo dust instrument between Venus and Mars orbit. *Journal of Geophysical Research*, 110:7102–7115.
- Altobelli, N., Kempf, S., Landgraf, M., Srama, R., Dikarev, V., Krüger, H., Moragas-Klostermeyer, G., and Grün, E. (2003). Cassini between Venus and Earth: Detection of Interstellar Dust. *Journal of Geophysical Research*, 108:A10, 7–1.
- Altobelli, N., Postberg, F., Fiege, K., Trieloff, M., Kimura, H., Sterken, V. J., Hsu, H.-W., Hillier, J., Khawaja, N., Moragas-Klostermeyer, G., Blum, J., Burton, M., Srama, R., Kempf, S., and Gruen, E. (2016). Flux and composition of interstellar dust at Saturn from Cassini’s Cosmic Dust Analyzer. *Science*, 352:312–318.
- Auer, S. (2001). Instrumentation. In Grün, E., Gustafson, B. A. S., Dermott, S. F., and Fechtig, H., editors, *Interplanetary Dust*, pages 385–444. Springer Verlag, Berlin Heidelberg New York.
- Baguhl, M., Grün, E., and Landgraf, M. (1996). In Situ Measurements of Interstellar Dust with the Ulysses and Galileo Spaceprobes. *Space Science Reviews*, 78:165–172.

- Belheouane, S., Zaslavsky, A., Meyer-Vernet, N., Issautier, K., Mann, I., and Maksimovic, M. (2012). Detection of Interstellar Dust with STEREO/WAVES at 1 AU. *Solar Physics*, 281:501–506.
- Bertaux, J. L. and Blamont, J. F. (1976). Possible evidence for penetration of interstellar dust into the solar system. *Nature*, 262:263–266.
- Dietzel, H., Eichhorn, G., Fechtig, H., Grün, E., Hoffmann, H. J., and Kissel, J. (1973). The HEOS 2 and HELIOS micrometeoroid experiments. *Journal of Physics E Scientific Instruments*, 6:209–217.
- Fechtig, H., Grün, E., and Kissel, J. (1978). Laboratory Simulation. In McDonnell, J. A. M., editor, *Cosmic Dust*, pages 607–669. Wiley.
- Frisch, P. C., Dorschner, J., Geiß, J., Greenberg, J. M., Grün, E., Landgraf, M., Hoppe, P., Jones, A. P., Krätschmer, W., Linde, T. J., Morfill, G. E., Reach, W. T., Slavin, J., Svestka, J., Witt, A., and Zank, G. P. (1999). Dust in the Local Interstellar Wind. *Astrophysical Journal*, 525:492–516.
- Göller, J. R. and Grün, E. (1985). Calibration of the GALILEO/ISPM Dust Detectors with Iron Particles. In Giese, R. H. and Lamy, P., editors, *Properties and Interaction of Interplanetary Dust*, pages 113–115. Reidel, Dordrecht.
- Göller, J. R. and Grün, E. (1989). Calibration of the GALILEO/ULYSSES dust detectors with different projectile materials and at varying impact angles. *Planetary and Space Science*, 37:1197–1206.
- Grün, E. (1981). Physikalische und chemische Eigenschaften der interplanetaren Staubmessungen des Mikrometeoroidenexperimentes auf Helios. Technical report, Bundesministerium für Forschung und Technologie, Forschungsbericht W 81-034.
- Grün, E., Baguhl, M., Hamilton, D. P., Kissel, J., Linkert, D., Linkert, G., and Riemann, R. (1995). Reduction of Galileo and Ulysses dust data. *Planetary and Space Science*, 43:941–951.
- Grün, E., Fechtig, H., Hanner, M. S., Kissel, J., Lindblad, B. A., Linkert, D., Maas, D., Morfill, G. E., and Zook, H. A. (1992a). The Galileo dust detector. *Space Science Reviews*, 60:317–340.
- Grün, E., Fechtig, H., Kissel, J., Linkert, D., Maas, D., McDonnell, J. A. M., Morfill, G. E., Schwehm, G. H., Zook, H. A., and Giese, R. H. (1992b). The Ulysses dust experiment. *Astronomy and Astrophysics, Supplement*, 92:411–423.
- Grün, E., Gustafson, B. E., Mann, I., Baguhl, M., Morfill, G. E., Staubach, P., Taylor, A., and Zook, H. A. (1994). Interstellar dust in the heliosphere. *Astronomy and Astrophysics*, 286:915–924.

- Grün, E., Staubach, P., Baguhl, M., Hamilton, D. P., Zook, H. A., Dermott, S. F., Gustafson, B. A., Fechtig, H., Kissel, J., Linkert, D., Linkert, G., Srama, R., Hanner, M. S., Polanskey, C., Horányi, M., Lindblad, B. A., Mann, I., McDonnell, J. A. M., Morfill, G. E., and Schwehm, G. H. (1997). South-North and Radial Traverses through the Interplanetary Dust Cloud. *Icarus*, 129:270–288.
- Grün, E., Zook, H. A., Baguhl, M., Balogh, A., Bame, S. J., Fechtig, H., Forsyth, R., Hanner, M. S., Horányi, M., Kissel, J., Lindblad, B. A., Linkert, D., Linkert, G., Mann, I., McDonnell, J. A. M., Morfill, G. E., Phillips, J. L., Polanskey, C., Schwehm, G. H., Siddique, N., Staubach, P., Svestka, J., and Taylor, A. (1993). Discovery of Jovian dust streams and interstellar grains by the Ulysses spacecraft. *Nature*, 362:428–430.
- Gustafson, B. A. S. (1994). Physics of Zodiacal Dust. *Annual Review of Earth and Planetary Sciences*, 22:553–595.
- Hoeksema, J. (2018). *Wilcox Solar Observatory*. <http://wso.stanford.edu>.
- Kawakatsu, Y. and Itawa, T. (2013). Destiny mission overview: a small satellite mission for deep space exploration technology demonstration. *Advances in the Astronautical Sciences*, 146:12–585, 13 pages.
- Kellogg, P. J., Goetz, K., and Monson, S. J. (2018). Are STEREO single hits dust impacts? *Journal of Geophysical Research*, 123:7211–7219.
- Kempf, S., Srama, R., Altobelli, N., Auer, S., Tschernjawski, V., Bradley, J., Burton, M. E., Helfert, S., Johnson, T. V., Krüger, H., Moragas-Klostermeyer, G., and Grün, E. (2004). Cassini between Earth and asteroid belt: first in-situ charge measurements of interplanetary grains. *Icarus*, 171:317–335.
- Kimura, H., Kobayashi, M., Wada, K., Arai, T., Ishiguro, M., Hanayama, H., Ishibashi, K., Hirai, T., Yoshida, F., and Hong, P. (2019). On the Detection of an Ejecta Dust Cloud around Asteroid (3200) Phaethon by the DESTINY⁺ Dust Analyzer. I. Blackbody Approximation. *Planetary and Space Science*. submitted.
- Kimura, H. and Mann, I. (1998). The Electric Charging of Interstellar Dust in the Solar System and Consequences for Its Dynamics. *Astrophysical Journal*, 499:454–462.
- Kimura, H. and Mann, I. (1999). Radiation pressure on porous micrometeoroids. In Baggaley, W. J. and Porubcan, V., editors, *Meteoroids 1998*, pages 283–286. Astronomical Institute of the Slovak Academy of Sciences.
- Kimura, H., Mann, I., and Jessberger, E. K. (2003). Composition, Structure, and Size Distribution of Dust in the Local Interstellar Cloud. *Astrophysical Journal*, 583:314–321.
- Krüger, H., Dikarev, V., Anweiler, B., Dermott, S. F., Graps, A. L., Grün, E., Gustafson, B. A., Hamilton, D. P., Hanner, M. M. S., Horányi, M., Kissel, J., Linkert, D., Linkert, G., Mann, I., McDonnell, J. A. M., Morfill, G. E., Polanskey, C.,

- Schwehm, G. H., and Srama, R. (2010). Three years of Ulysses dust data: 2005 to 2007. *Planetary and Space Science*, 58:951–964.
- Krüger, H., Graps, A. L., Hamilton, D. P., Flandes, A., Forsyth, R. J., Horányi, M., and Grün, E. (2006). Ulysses jovian latitude scan of high-velocity dust streams originating from the jovian system. *Planetary and Space Science*, 54:919–931.
- Krüger, H. and Grün, E. (2009). Interstellar dust inside and outside the heliosphere. In Linsky, J. and Izmodenov, V. and Möbius, E., editor, *From the outer heliosphere to the local bubble*. Springer Heidelberg.
- Krüger, H., Landgraf, M., Altobelli, N., and Grün, E. (2007). Interstellar dust in the solar system. *Space Science Reviews*, 130:401–408.
- Krüger, H., Strub, P., Srama, R., Kobayashi, M., Arai, T., Kimura, H., Moragas-Klostermeyer, G., Altobelli, N., Sterken, V., Agarwal, J., Sommer, M., and Grün, E. (2019). Modelling destiny⁺ interplanetary and interstellar dust measurements en route to the active asteroid (3200) phaethon. *Planetary and Space Science*. submitted.
- Krüger, H., Strub, P., Sterken, V. J., and Grün, E. (2015). Sixteen years of ulysses interstellar dust measurements in the solar system: I. mass distribution and gas-to-dust mass ratio. *Astrophysical Journal*, 812:139.
- Landgraf, M. (1998). *Modellierung der Dynamik und Interpretation der In-situ-Messung interstellaren Staubs in der lokalen Umgebung des Sonnensystems*. PhD thesis, Ruprecht-Karls-Universität Heidelberg.
- Landgraf, M. (2000). Modelling the Motion and Distribution of Interstellar Dust inside the Heliosphere. *Journal of Geophysical Research*, 105, no. A5:10,303–10316.
- Landgraf, M., Augustsson, K., Grün, E., and Gustafson, B. A. S. (1999). Deflection of the local interstellar dust flow by solar radiation pressure. *Science*, 286:2,319–2,322.
- Landgraf, M., Baggeley, W. J., Grün, E., Krüger, H., and Linkert, G. (2000). Aspects of the Mass Distribution of Interstellar Dust Grains in the Solar System from in situ Measurements. *Journal of Geophysical Research*, 105, no. A5:10,343–10352.
- Landgraf, M., Krüger, H., Altobelli, N., and Grün, E. (2003). Penetration of the Heliosphere by the interstellar dust stream during solar maximum. *Journal of Geophysical Research*, 108:5–1.
- Malaspina, D. M. and Wilson, L. B. (2016). A database of interplanetary and interstellar dust detected by the Wind spacecraft. *Journal of Geophysical Research*, 121:9369–9377.
- Mann, I. (2010). Interstellar Dust in the Solar System. *Annual Review of Astronomy and Astrophysics*, 48:173–203.

- McComas, D. J., Bzowski, M., Fuselier, S. A., Frisch, P. C., Galli, A., Izmodenov, V. V., Katushkina, O. A., Kubiak, M. A., Lee, M. A., Leonard, T. W., Möbius, E., Park, J., Schwadron, N. A., Sokol, J. M., Swaczyna, P., Wood, B. E., and Wurz, P. (2015). Local interstellar medium: Six years of direct sampling by ibex. *Astrophysical Journal, Supplement*, 220:22.
- Slavin, J. D., Frisch, P. C., Müller, H.-R., Heerikhuisen, J., Pogorelov, N. V., Reach, W. T., and Zank, G. (2012). Trajectories and Distribution of Interstellar Dust Grains in the Heliosphere. *Astrophysical Journal*, 760:46.
- Srama, R. (2009). *Cassini-Huygens and Beyond - Tools for Dust Astronomy*. Habilitation Thesis. Universität Stuttgart.
- Srama, R., Ahrens, T. J., Altobelli, N., Auer, S., Bradley, J. G., Burton, M., Dikarev, V. V., Economou, T., Fechtig, H., Görlich, M., Grande, M., Graps, A. L., Grün, E., Havnes, O., Helfert, S., Horányi, M., Igenbergs, E., Jeßberger, E. K., Johnson, T. V., Kempf, S., Krivov, A. V., Krüger, H., Moragas-Klostermeyer, G., Lamy, P., Landgraf, M., Linkert, D., Linkert, G., Lura, F., Mockler-Ahlreep, A., McDonnell, J. A. M., Möhlmann, D., Morfill, G. E., Müller, M., Roy, M., Schäfer, G., Schlotzhauer, G. H., Schwehm, G. H., Spahn, F., Stübig, M., Svestka, J., Tschernjawski, V., Tuzzolino, A. J., Wäsch, R., and Zook, H. A. (2004). The Cassini Cosmic Dust Analyzer. *Space Science Reviews*, 114:465–518.
- Sterken, V. J., Altobelli, N., Kempf, S., Krüger, H., Srama, R., Strub, P., and Grün, E. (2013). The filtering of interstellar dust in the solar system. *Astronomy and Astrophysics*, 552:A130.
- Sterken, V. J., Altobelli, N., Kempf, S., Schwehm, G., Srama, R., and Grün, E. (2012). The flow of interstellar dust into the solar system. *Astronomy and Astrophysics*, 538:A102.
- Sterken, V. J., Strub, P., Krüger, H., von Steiger, R., and Frisch, P. (2015). Sixteen years of Ulysses Interstellar Dust Measurements in the Solar System: III. Simulations and Data unveil new insights into Local Interstellar Dust. *Astrophysical Journal*, 812:141.
- Sterken, V. J., Westphal, A. J., N., A., D., M., and P., F. (2019). Interstellar Dust in the Solar System. *Space Science Reviews*. in press.
- Strub, P., Krüger, H., and Sterken, V. J. (2015). Sixteen years of Ulysses interstellar dust measurements in the Solar System: II. Fluctuations in the dust flow from the data. *Astrophysical Journal*, 812:140.
- Strub, P., Sterken, V. J., Soja, R., Krüger, H., Grün, and Srama, R. (2019). Heliospheric modulation of the interstellar dust flow on to Earth. *Astronomy and Astrophysics*, 621:A54.

- Stübig, M. (2002). *New insights in impact ionization and in time-of-flight mass spectroscopy with micrometeoroid detectors by improved impact simulations in the laboratory*. PhD thesis, Ruprecht-Karls-Universität Heidelberg.
- Swaczyna, P., Bzowski, M., Kubiak, M. A., Sokół, J. M., Fuselier, S. A., Galli, A., Heirtzler, D., Kucharek, H., McComas, D. J., Möbius, E., Schwadron, N. A., and Wurz, P. (2018). Interstellar Neutral Helium in the Heliosphere from IBEX Observations. V. Observations in IBEX-Lo ESA Steps 1, 2, and 3. *Astrophysical Journal*, 854:119.
- Szalay, J.-R., Pokorny, P., Horányi, M., Janches, D., Sarantos, M., and Srama, R. (2019). Impact Ejecta Environment of an Eccentric Asteroid: 3200 Phaethon. *Planetary and Space Science*, 165:194–204.
- Westphal, A. J., Stroud, R. M., Bechtel, H. A., Brenker, F. E., Butterworth, A. L., Flynn, G. J., Frank, D. R., Gainsforth, Z., Hillier, J. K., Postberg, F., Simionovici, A. S., Sterken, V. J., Nittler, L. R., Allen, C., Anderson, D., Ansari, A., Bajt, S., Bastien, R. K., Bassim, N., Bridges, J., Brownlee, D. E., Burchell, M., Burghammer, M., Changela, H., Cloetens, P., Davis, A. M., Doll, R., Floss, C., Grün, E., Heck, P. R., Hoppe, P., Hudson, B., Huth, J., Kearsley, A., King, A. J., Lai, B., Leitner, J., Lemelle, L., Leonard, A., Leroux, H., Lettieri, R., Marchant, W., Ogliore, R., Ong, W. J., Price, M. C., Sandford, S. A., Sans Tresseras, J. A., Schmitz, S., Schoonjans, T., Schreiber, K., Silversmit, G., Solé, V. A., Srama, R., Stadermann, F. J., Stephan, T., Stodolna, J., Sutton, S., Tieloff, M., Tsou, P., Tyliczszak, T., Vekemans, B., Vincze, L., Von Korff, J., Wordsworth, N., Zevin, D., Zolensky, M. E., and 30714 Stardust@home dusters (2014). Evidence for interstellar origin of seven dust particles collected by the Stardust spacecraft. *Science*, 345:786–791.
- Witte, M., Banaszekiewicz, H., and Rosenbauer, H. (1996). Recent results on the parameters of interstellar helium from the Ulysses/GAS experiment. *Space Science Reviews*, 78, no. 1/2:289–296.
- Witte, M., Banaszekiewicz, M., Rosenbauer, H., and McMullin, D. (2004). Kinetic parameters of interstellar neutral helium: updated results from the Ulysses/GAS instrument. *Advances in Space Research*, 34:61–65.
- Wolf, H., Rhee, J., and Berg, O. E. (1976). Orbital elements of dust particles intercepted by Pioneers 8 and 9. In Elsässer, H. and Fechtig, H., editors, *Interplanetary Dust and Zodiacal Light*, volume 48 of *Lecture Notes in Physics*, Berlin Springer Verlag, pages 165–169.
- Wood, B. E., Müller, H.-R., and Witte, M. (2015). Revisiting Ulysses Observations of Interstellar Helium. *Astrophysical Journal*, 801:62+.